Single Molecule Modulation Spectroscopy of Conjugated Polymers

ARTICLE *in* THE JOURNAL OF PHYSICAL CHEMISTRY B · JULY 2005

Impact Factor: 3.3 · DOI: 10.1021/jp0507851 · Source: PubMed

4 AUTHORS, INCLUDING:

Andre J Gesquiere
University of Central Florida
43 PUBLICATIONS **1,034** CITATIONS
SEE PROFILE

Young Jong Lee
National Institute of Standards and Technolo…
46 PUBLICATIONS **918** CITATIONS
SEE PROFILE

Single Molecule Modulation Spectroscopy of Conjugated Polymers

Andre J. Gesquiere, Young Jong Lee, Ji Yu, and Paul F. Barbara*

Center for Nano- and Molecular Science and Technology and Department of Chemistry and Biochemistry, University of Texas, Austin, Texas 78712

Received: February 14, 2005; In Final Form: May 4, 2005

This paper describes a new single molecule spectroscopy approach for the investigation of triplet−triplet and singlet−triplet interactions in conjugated polymers. The technique involves the irradiation of isolated single, mulitchromophoric, conjugated polymer molecules by a repetitive sequence of variable-intensity microsecond time scale excitation pulses. The fluorescence intensity is synchronously time-averaged for thousands of cycles of the pulse sequence to yield a high signal-to-noise fluorescence transient on the microsecond time scale. The transient can be analyzed with kinetic models to obtain quantitative information about the kinetics of triplet−triplet exciton annihilation and the quenching of singlet excitons by triplet excitons in conjugated polymers.

I. Introduction

Singlet and triplet excitons in conjugated polymers can play an important role in many promising applications of these materials, e.g., in luminescence organic light-emitting displays (OLEDs), solar cells, and chemical sensors.[1−8] While a great deal is understood about singlet excitons in conjugated polymers, much less is known about triplet excitons. Triplet excitons are more difficult to study for two main reasons. First, triplets are nonemissive or "dark" and as a result cannot usually be directly observed by emission spectroscopy. Second, since triplet excitons have orders-of-magnitude longer lifetimes than singlets, triplet excitons are more likely than singlets to interact with such species as excitons, polarons, impurities, etc., through various chemical reactions and quenching processes. This could in principle significantly degrade the performance of a device based on excitons.[9−13] Triplet−triplet annihilation and the quenching of triplets by polarons are also important since they can strongly affect the steady-state triplet concentration and the migration length of triplet excitons, both of which can have important implications for device performance.[14−20]

Recently, we have demonstrated that single molecule spectroscopy[21−40] (SMS) has several advantages for the investigation of the triplet photodynamics of conjugated polymers.[41] The SMS approach has yielded new measurements for specific rate constants and yields for critical bimolecular processes involving triplet excitons in conjugated polymers, e.g., the quenching of singlet excitons by triplet excitons. The previously obtained SMS data (for single multichromophoric molecules of the conjugated MEH−PPV polymers {poly[2-methoxy-5-(2′-ethylhexyloxy)-*p*-phenylene vinylene]} and F8BT [poly(9,9′-dioctylfluorene cobenzothiadiazole)]) demonstrate for these polymers that (i) triplet exciton pairs undergo efficient triplet−triplet annihilation on the $\ll$30 μs time scale, (ii) triplet−triplet annihilation is the dominant mechanism for triplet decay at incident excitation intensities of $\geq$50 W/cm^2, and (iii) singlet excitons are efficiently quenched (>50%) by triplet excitons, allowing for an indirect observation of triplets via quenching of the fluorescence of the singlet excitons. Assuming an initial concentration of one triplet per molecule, our assumption of triplet−triplet annihilation on the $\ll$30 μs time scale gives an estimated second-order rate constant of $> 3 \times 10^{-14}$ cm^3 s^{-1}. This is in reasonable agreement with the triplet−triplet annihilation rate that has been previously measured for MEH−PPV in thin films ($\cong 10^{-14}$ cm^3 s^{-1}).[14]

Only a small number of photons are detected during the short duration of the formation and decay of a triplet exciton in a conjugated polymer. Thus, the signal-to-noise ratio in an emission transient, $F(t)$, is too small to allow for the real time intensity observation $F(t)$ of "triplet blinking" with an acceptable signal-to-noise ratio. Instead, we have recently shown that intensity autocorrelation analysis of the micro- to millisecond dynamics of conjugated polymers

$$G(\tau) = \frac{\langle F(t)F(t+\tau)\rangle}{\langle F\rangle^2} - 1 \qquad (1)$$

can be used to statistically characterize the triplet dynamics of these materials.[41,42] Using this approach, $G(\tau)$ data have been acquired for a specific molecule at a set of different irradiation intensities. A global analysis of the set of $G(\tau)$ data for each molecule (in terms of a multichromophoric kinetic model) has allowed for a determination of the triplet−triplet and singlet−triplet interaction rate constants. Despite the usefulness of this approach, it does have certain practical limitations. The autocorrelation analysis is highly susceptible to errors due to background light, dark noise, and "detector after pulsing". Furthermore, the autocorrelation data are less straightforward to analyze than data from conventional time-resolved spectroscopies.

This paper describes an alternative technique for studying triplet dynamics in multichromophoric molecules, namely, single molecule excitation intensity modulation spectroscopy. In this approach, the fluorescence intensity $F(t)$ of a single-conjugated polymer molecule is recorded while irradiating the molecule with many repetitive cycles of a sequence of sub-millisecond time scale excitation pulses of varying intensity. Synchronous averaging of $F(t)$ yields time ensemble intensity $F(t')$ versus t' curves, where t' refers to time within the cycle.

* To whom correspondence should be addressed. E-mail: p.barbara@mail.utexas.edu.

10.1021/jp0507851 CCC: $30.25
Published on Web 06/02/2005

$F(t')$ data can be analyzed to determine the kinetics of triplet formation and decay as a function of the time history of the irradiation. The new technique is applied herein in investigating the triplet dynamics of MEH−PPV and F8BT, and the results are compared to previous intensity autocorrelation studies of triplet dynamics for these conjugated polymers. In addition, a recently introduced kinetic model for triplet dynamics in conjugated polymers is adapted for the analysis of the single-molecule modulation data.

II. Experimental Section

Experimental samples were comprised of a glass microscope coverslip that was coated with a 100−300 nm spin-coated polymer film comprised of an inert host polymer (polymethyl methacrylate or polystyrene) that contained a very low concentration ($\sim 10^{-11}$ M) of conjugated polymer molecules. A metal layer (Au or Al, ~100 nm thick) was evaporated on top of the host polymer film to exclude oxygen, which has been shown to efficiently quench triplet states in polymer thin films. MEH−PPV was obtained from Uniax Corp. F8BT was synthesized by Cambridge Display Technology and kindly provided by the Friend group (Cavendish Laboratory, University of Cambridge, Cambridge, U.K.).

The experimental apparatus is a home-built sample scanning confocal microscope. Emission is detected by an avalanche photodiode (APD) (Perkin-Elmer Optoelectronics, model SPCM-AQR-15). The transient signal $F(t)$ from the detector is recorded with a multichannel scalar (MCS) that was synchronized to the sequence of excitation pulses. The sequence of excitation pulses $I_E(t)$ was derived from the output of an argon ion laser (514 nm or alternatively 488 nm for MEH−PPV and 458 nm for F8BT) that was intensity-modulated by an acoustic optical modulator (IntraAction Corp., model AOM-40). The input electronic waveform to the modulator was produced by a programmable function generator (Wavetek, model 29) that was synchronized to the MCS. Two different MCS boards were used: a home-built MCS based on a counter board in a personal computer and a shorter time scale, commercial MCS (FAST ComTec Gmbh, model MCA-3).

III. Results

This paper is focused on the fluorescence dynamics of single MEH−PPV and F8BT molecules irradiated by a repetitive sequence of excitation pulses. In a typical experiment, a confocal fluorescence intensity image was acquired to locate the single molecules in the range of the scanning stage. To record an emission transient, the sample was translated such that a single molecule was in the focus of the microscope, and then the molecule was exposed to a time varying excitation intensity $I_E(t)$ while the emission transient $F(t)$ was simultaneously recorded. Figure 1A exhibits representative data for the fluorescence intensity versus time [$F(t)$] of a single MEH−PPV molecule irradiated by a repetitive sequence of 500 μs excitation pulses (Figure 1B). Because of the high stability of conjugated polymers in the oxygen-depleted environments of these films, $F(t)$ can typically be acquired for hundreds of seconds, corresponding to hundreds of thousands of cycles of the excitation pulse sequence. These data contain information about the triplet formation and decay kinetics, but the limited signal-to-noise ratio (due to photon shot noise) completely obscures these kinetics. During the "on" period, the irradiation light has a power of 3.2 μW, which corresponds to a peak intensity of the focused

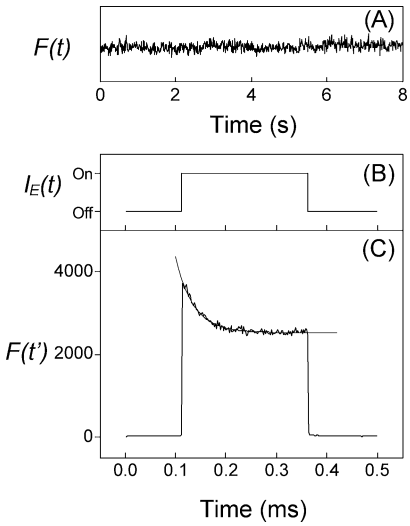

Figure 1. (A) Fluorescence intensity [$F(t)$] trajectory of a single MEH−PPV molecule irradiated by a repetitive sequence of excitation pulses. (B) A square wave modulation of the excitation laser intensity is applied. (C) A synchronously time-averaged fluorescence trajectory [$F(t')$] comprised of many cycles is shown. The initial intensity when the laser is turned on drops to a lower steady-state level due to the buildup of a triplet population that quenches the singlet excited-state emission. These data fit well with a single-exponential function (gray line). The relaxation time τ extracted from the fit is 36 μs.

laser spot of 2.3 kW/cm^2 at the sample. This was calculated from the average power during the on period based on a Gaussian intensity profile and a measured spot size of 350 nm.

Synchronous averaging of the data over tens to hundreds of seconds yields a high signal-to-noise time-ensemble transient [$F(t')$] that reflects the irradiation pulse-induced kinetics of triplet formation and/or decay, as shown in Figure 1C. The $F(t')$ fluorescence intensity data are at the dark noise level during the portion of the cycle when the irradiation pulse is off, and then within the time resolution of the experiment, $F(t')$ "jumps" to a peak value. The intensity decays during the irradiation pulse to a constant "plateau". The decay is fit well by a single-exponential decay in most cases, leading to the following empirical form for $F(t')$ for each pulse period

$$F(t') \propto R\mathrm{e}^{-t'/\tau} + 1 \qquad (2)$$

where τ is the relaxation time and R is the amplitude of the exponential response. The data in Figure 1 were fitted (gray line) to this function. The relaxation time τ extracted from the fit is 36 μs. The data for both MEH−PPV and F8BT are fit well by eq 2 over a large range of excitation intensities (0.1−4.0 kW/cm^2).

Analogous $F(t')$ transients were observed for hundreds of different single molecules of the conjugated polymers MEH−PPV and F8BT for a broad range of irradiation intensities. The observed $F(t')$ data do not vary as a function of the specific time region used in the synchronous averaging, demonstrating that the $F(t')$ transient is a steady-state response of the single molecule to the repetitive pulse sequence. In general, the observed τ values decrease as the excitation power is increased. In contrast, the observed R values increase as the excitation intensity is increased until they reach a constant value at high power.

Kinetic modeling (see below) demonstrates that the observed $F(t')$ behavior is a straightforward consequence of the combined effect of triplet−triplet annihilation and singlet quenching by triplets in the conjugated polymers. During the excitation off

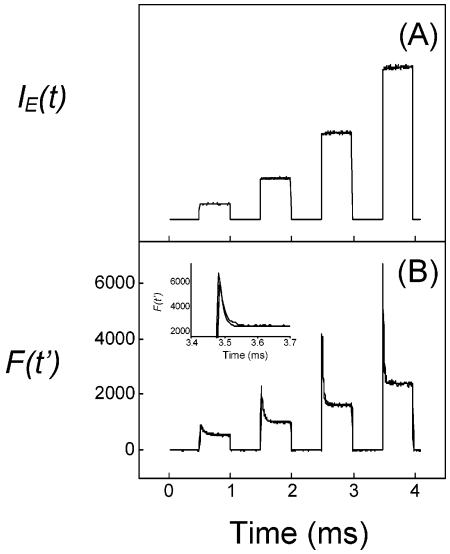

Figure 2. Time-averaged fluorescence transient of a single MEH−PPV molecule acquired while modulating the excitation laser intensity. (A) A cycle containing four excitation windows, each with a different excitation intensity, is repeatedly applied to a selected single molecule. From left to right, the excitation powers are 0.2, 0.5, 0.8, and 1.2 kW/cm^2 at the sample, respectively. (B) The synchronously time-averaged fluorescence trajectory comprised of many cycles is shown. The contrast between the initial fluorescence intensity and steady-state fluorescence intensity within an excitation window increases with an increase in excitation intensity (from left to right) due to an increasing triplet exciton population. The gray line is a result of fitting the data to the kinetic model described in this paper. The inset shows a zoom of the top part of the fourth excitation window (right) and shows that the data are fit well by the model.

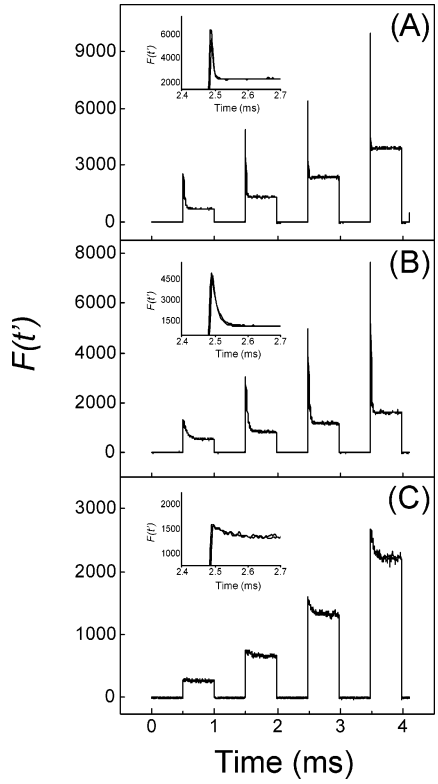

Figure 3. Intensity modulation data for three different MEH−PPV single molecules, plotted with their fits to the kinetic model described in this paper (gray lines). These data show that all MEH−PPV molecules qualitatively exhibit the same behavior, i.e., increasing contrast and decay rate with increasing excitation intensity. They differ quantitatively due to molecule to molecule variations in the ensemble of molecules. The insets show a zoom of the top part of the third excitation window and show that the data are fit well by the model.

period, triplet excitons decay due to reverse intersystem crossing ($T_1 \rightarrow S_0$) with a rate constant signified by k'_{isc}. For the various data in this paper, the off periods are sufficiently long to significantly reduce the triplet exciton populations, and in most cases, the triplet population is close to zero before the next irradiation pulse. Immediately after the excitation pulse is turned on, the emission $F(t')$ reflects the emission of an essentially triplet free molecule. As time progresses, multiple excitations ($S_0 \rightarrow S_1$) occur, causing a buildup of triplet excitons as a result of forward intersystem crossing ($S_1 \rightarrow T_1$). The increase in the fractional triplet population (the probability of having one triplet on the polymer chain) is reflected in the decay of $F(t')$. The fluorescence intensity decreases as the triplet population increases due primarily to singlet quenching by triplets ($S_1 + T_1 \rightarrow S_0 + T_1$) in the multichromophoric conjugated polymer molecule. Due to triplet−triplet annihilation ($T_1 + T_1 \rightarrow S_1 + S_0$), however, the triplet population reaches a steady-state population, which corresponds to the plateau in the $F(t')$ data during the on period of the laser.

Figure 2 portrays data from an alternative, more advanced SMS modulation technique for investigating triplet dynamics in conjugated polymers. This variation of the basic modulation experiment involves a pulse sequence that includes several pulses of different intensity within an irradiation pulse cycle. For Figure 2, a single MEH−PPV molecule was exposed to a repeating sequence of four irradiation pulses of different intensities, i.e., 0.2, 0.5, 0.8, and 1.2 kW/cm^2. These data demonstrate that the contrast ratio R increases as the irradiation pulse intensity is increased due to a larger population of triplet excitons at higher irradiation intensities. Furthermore, these data parallel fluorescence intensity autocorrelation measurements for MEH−PPV, which show that the amplitude of the correlation function $G(\tau)$ also increases with excitation intensity as a result of an increasing triplet population with increasing excitation intensity.[41] The type of experiment in Figure 2 was reproduced for several MEH−PPV molecules as shown in Figure 3, yielding qualitatively similar trends but different quantitative behaviors reflecting molecule to molecule variations of the relevant photophysical parameters.

IV. Photodynamic Model

Isolated molecules of the conjugated polymers investigated herein (MEH−PPV and F8BT) are known to behave as multichromophoric molecular systems due to a distribution of conjugated segments on the polymer chain (connected by chemical and structural defects). For the MEH−PPV molecules in this study (MW $\sim 10^6$), there are $\sim$200 effective chromophores, each with $\sim$10 repeat units in conjugation length, in a single molecule, while for the F8BT molecules in this study (MW $\sim 10^5$), there are $\sim$50 effective chromophores, each with $\sim$4−5 repeat units in conjugation length, in a single molecule.

The observed $F(t')$ data are highly consistent with predictions from the recently developed kinetic population-state model for multichromophoric conjugated polymers.[41] In this model, we assume that the photodynamics are described well by a set of first-order incoherent rate processes. These processes connect population states of the system that correspond to each chromophore occupying S_0, S_1, and T_1 at a given time. A simple example is the intersystem crossing in a molecule with four weakly coupled chromophores: (S_0, S_1, S_0, S_0) $\rightarrow$ (S_0, T_1, S_0, S_0). An additional assumption is made: only the number of each type of excitation matters, not the specific configuration of these

excitations in the polymer chain. This approximation would be valid, for example, if triplet exciton diffusion was sufficiently rapid to ensure "homogeneous" kinetics and there was a narrow distribution of site energies. In this case, we can describe the excited states of conjugated polymer single molecules in terms of localized excitons, i.e., $(N_S, N_T) \rightarrow (N_{S'}, N_{T'})$, where N_S, N_T, $N_{S'}$, and $N_{T'}$ are the number of singlet and triplet excitons in the entire chain before and after the specific photophysical process, respectively. Due to an assumption of very rapid triplet−triplet annihilation (see section I) and a separation of time scales for the fast (singlet−singlet annihilation, internal conversion, and emission of fluorescence) and slow (reverse intersystem crossing and formation of a triplet via $S_0 \rightarrow S_1$ followed by intersystem crossing at low to moderate excitation rates) processes, the conjugated polymer is predicted to spend most of the time in either (0,0) or (0,1) states. Correspondingly, the population kinetic scheme reduces to an approximate two-state model

$$(0,0) \underset{k_B}{\overset{k_F}{\rightleftharpoons}} (0,1) \tag{3}$$

with opposing forward and backward first-order rate constants, k_F and k_B, respectively, that are given by

$$k_F = k_{exc} k_{isc} \tau_{fl} \tag{4}$$

$$k_B = k'_{isc} + k_{exc} k_{isc} \tau'_{fl} \tag{5}$$

where k'_{isc} is the reverse ISC rate, k_{isc} is the ISC rate, τ_{fl} is the fluorescence lifetime of the (1,0) state, and τ'_{fl} is the fluorescence lifetime of the (1,1) state, which can be significantly shorter than τ_{fl} because of an additional relaxation process for (1,1), namely, singlet-induced quenching by a triplet exciton. This two-state model for conjugated polymers corresponds with a simple single-exponential decaying $F(t')$ (see eqs 2 and 10) where $(\tau)^{-1} = k = k_F + k_B$. The excitation rate k_{exc} is given by

$$k_{exc} = \frac{I_E(t)\sigma}{h\nu} \tag{6}$$

where $I_E(t)$ is the incident excitation intensity, σ the absorption cross section of the molecule, and $h\nu$ the energy of the photons.

In this model, the effect of singlet quenching by triplets is quantified by the rate constant for singlet quenching by a triplet in a single molecule (k_{QST}):[41]

$$k_{QST} = \frac{1}{\tau'_{fl}} - \frac{1}{\tau_{fl}} \tag{7}$$

Through previously reported work, it has been shown that other quenchers besides triplets can be ruled out.[41] In the presence of oxygen, which efficiently quenches triplets, the intensity dynamics reported herein are not observed. This observation was also corroborated by autocorrelation experiments on unsealed samples before and during the flowing of a stream of argon gas.[41]

Although we do not rule out the possibility of a Dexter-type mechanism, the quenching of singlets by triplets mainly occurs via a Forster energy transfer process. The singlet−triplet Forster energy transfer rate (k_{ST}) was calculated on the basis of the MEH−PPV emission spectrum of an ensemble of single molecules and the transient absorption spectrum of MEH−PPV triplets. k_{ST} was calculated to be $\sim 10^{10}$ s^{-1}, which is in good agreement with the values for k_{QST} that are reported in Table 1. The large molecule to molecule variation reflects the conformational heterogeneity in the ensemble of single molecules. The conformation of the molecules is mostly a defect cylinder, in which extended conjugated segments are folded on top of each other.[43] Some of these segments will contact each other, leading to the formation of low-energy chromophores toward which excitation energy is efficiently funneled. Small molecule to molecule variations in this conformation of the polymer chains can lead to differences in energy funneling efficiency when comparing molecules, and can account for the observed heterogeneity in energy transfer rates.

TABLE 1: Absorption Cross Sections (σ), Rate Constants for Reverse Intersystem Crossing (k'_{isc}), and Rate Constants for Quenching of Singlets by Triplets (k_{QST}) Determined for Several MEH−PPV Molecules through Kinetic Simulations

molecule	σ (cm^2)	k'_{isc} (s^{-1})	k_{QST} (s^{-1})	Figure
MEH−PPV	7.4×10^{-16}	5.0×10^3	2.7×10^9	3C
MEH−PPV	2.4×10^{-14}	5.0×10^3	6.4×10^{10}	3A
MEH−PPV	4.4×10^{-15}	8.0×10^3	3.0×10^{10}	2
MEH−PPV	9.9×10^{-15}	10.0×10^3	1.3×10^{10}	*a*
MEH−PPV	1.0×10^{-14}	8.0×10^3	3.0×10^{10}	*a*
MEH−PPV	6.7×10^{-15}	6.0×10^3	8.0×10^{10}	3B
F8BT	−	$1.5 \times 10^{3\,b}$	$4.9 \times 10^{8\,c}$	4

[a] Molecule not shown. [b] From ref 41. [c] Calculated from eqs 7 and 12 in the high-power regime.

V. Modeling of the Experimental Results

Contact of the photodynamic model to experiment is available through a solution of the differential equation under conditions of excitation by the repetitive sequence of excitation pulses corresponding to the time-varying excitation intensity, $I_E(t)$, e.g., Figure 2.

$$\frac{dP_1}{dt} = k_F P_1 - k_B(1 - P_1) \tag{8}$$

where P_1 is the time-dependent probability of occupying the (0,1) state in response to $I_E(t)$, the latter of which via eqs 4 and 5 causes a modulation in k_F and k_B. The fluorescence intensity within this model is given by

$$F(t') = \chi I_E(t')\{[1 - P_1(t)] + f[P_1(t)]\} \tag{9}$$

where χ is a product of various factors, such as the instrumental sensitivity, the quantum yield of the (1,0) state, and the cross section for absorption for the molecule, etc., $I_E(t')$ is the time-ensemble excitation intensity, and f is the ratio between the lifetimes of the (1,1) and (1,0) states, i.e., τ'_{fl}/τ_{fl}.

To correspond to the experimental situation, which involves signal averaging for thousands of cycles of the excitation intensity, the "long-time behavior" of eq 8 is required. To find this solution, it is useful to recognize that the experimental sequence includes one or more long time regions for which the excitation intensity is sufficiently high to allow for a buildup of a steady-state triplet population $P(t)$ $\{P(t) \rightarrow K(t)/[1 + K(t)]$, where $K(t) = k_F(t)/k_B(t)\}$. Thus, the long-time behavior of the solution to eq 9 is achieved after only one cycle of the pulse sequence.

During periods in the sequence at which the irradiation intensity is constant, the kinetic scheme implied by eqs 3−9 is analogous to a simple first-order reversible process for the time-dependent probabilities for the (0,0) and (0,1) states. This leads

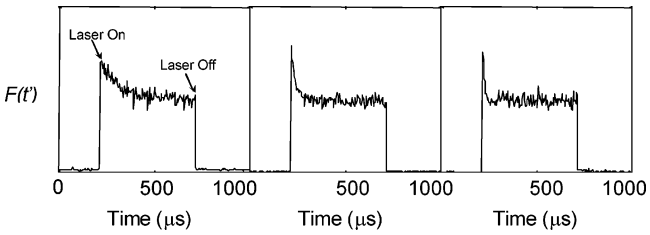

Figure 4. Intensity modulation data acquired for the same F8BT molecule at three different excitation intensities (from left to right, 0.1, 1.3, and 3.6 kW/cm^2, respectively). The fluorescence intensity for each panel is normalized to the peak intensity for each excitation power.

to the following simple prediction for each constant irradiation period:

$$F(t') = \chi(Ae^{-t'/\tau} + B) \tag{10}$$

$$1/\tau = k_F + k_B = k'_{isc} + k_{exc}k_{isc}(\tau_{fl} + \tau'_{fl}) \tag{11}$$

where A, B, and τ are parameters that can be easily determined by solving the kinetic scheme using the on and off duration for the pulse sequence, and chosen values for the various rate constants. Note that from eq 10 A, B, and τ can be directly compared to experiment (i.e., eq 2) for each pulse period using the relationship $R = A/B$.

A particularly simple case of this model is one in which there is a sufficiently long wait-time between irradiation pulses such that the prepulse triplet population P_T is approximately zero. This applies to wait times $\gg (k'_{isc})^{-1}$. For this "long wait" approach, the contrast ratio R_{lw} is given in this limit by

$$(R_{lw})^{-1} = 1 - \frac{k_{exc}k_{isc}(\tau_{fl} - \tau'_{fl})}{k'_{isc} + k_{exc}k_{isc}(\tau_{fl} + \tau'_{fl})} \tag{12}$$

allowing for a simple comparison with experiment.

The long wait approach, however, uses instrument time inefficiently since the laser pulse is off for a large fraction of the data collection time. Alternatively, R can be extracted from the data using shorter wait times between pulses, and a comparison can be made by directly fitting the solution of eq 9 to the observed $F(t')$ data. Figures 2 and 3 compare global fits of the kinetic models to the data for each single molecule of MEH−PPV at the various pulse powers. The model clearly captures the main observed trends in the data, strongly supporting the basic physics of the model. In addition, the parameters extracted from the modulation data (Table 1) are in reasonable agreement with the parameters extracted by the autocorrelation technique.[41] The data in Table 1 clearly illustrate the necessity of single molecule spectroscopy in developing a deep understanding of the photophysics of conjugated polymers. The observed heterogeneity in the ensemble of single molecules is a direct consequence of variations in the conformation of the molecules (see section IV).[43]

Figure 4 shows that the behavior of R in $F(t')$ versus $I_E(t')$ data behavior for F8BT is qualitatively different from that observed for MEH−PPV. For F8BT, R is independent of excitation intensity in the accessible excitation intensity range, i.e., >50 W/cm^2, while for MEH−PPV, R increases over this excitation intensity range. The kinetic model described above accounts well for this behavior. For F8BT, this effect is a consequence of the fact that at high excitation intensity both the forward (0,0) → (0,1) and reverse (0,1) → (0,0) processes are linearly proportional to the rate of generation of triplets ($k_{exc}k_{isc}\tau_{fl}$). Since at high excitation intensity $k'_{isc} \ll k_{exc}k_{isc}\tau'_{fl}$, the reverse intersystem crossing rate is much slower than the rate of triplet−triplet annihilation, and the annihilation process dominates. In contrast, the change in R as a function of irradiation power for MEH−PPV indicates that for this compound, k'_{isc} is comparable in magnitude to $k_{exc}k_{isc}\tau'_{fl}$ over the relevant excitation power range. The main reason for this difference between MEH−PPV and F8BT is the much greater rate constant for singlet quenching by triplets (k_{QST}) for MEH−PPV. The underlying reason for the difference in k_{QST} for MEH−PPV and F8BT is the difference in size between these molecules. The F8BT studied herein is a smaller molecule than the MEH−PPV that was studied. As discussed above, triplet−triplet annihilation is the dominating mechanism for triplet depopulation in F8BT even at very low excitation intensities, while MEH−PPV requires higher excitation intensities to reach this regime. This in turn accounts for higher fractional triplet populations in MEH−PPV and consequently a higher k_{QST}. The same conclusions for the contrasting behavior of F8BT and MEH−PPV have been reached from intensity autocorrelation studies of F8BT as a function of irradiation power. For F8BT, the contrast ratio of $G(\tau)$ was also observed to be constant over a large range of irradiation intensities.[41]

VI. Conclusions and Summary

A new technique that allows measurements of photophysical processes involving triplet excitons in multichromophoric molecules has been described in this paper. This technique involves the irradiation of isolated single, mulitchromophoric, conjugated polymer molecules by a repetitive sequence of variable-intensity microsecond time scale excitation pulses and results in a synchronously time-averaged high signal-to-noise fluorescence transient on the microsecond time scale. The data represent a decay of the time-averaged fluorescence intensity to a steady-state intensity, which corresponds with a buildup of a triplet exciton population in the conjugated polymer. These data can be analyzed with conventional deterministic kinetic models. The model that satisfactorily describes the experimental observations reduces the photophysics of the studied multichromophoric conjugated polymers to a simple two-state model. Quantitative information about the kinetics of triplet−triplet exciton annihilation and the quenching of singlet excitons by triplets in conjugated polymers has been obtained using this newly developed approach.

Characteristic observations were made for both MEH−PPV and F8BT concerning the observed contrast ratios and relaxation rates. For F8BT, the contrast ratio is independent of excitation power while the relaxation rate increases with excitation power. In the case of MEH−PPV, the contrast ratio and relaxation rate increase with excitation power in the power range that was used. These observations are consistent with an increasing triplet concentration on the molecules with increasing excitation intensity. For F8BT, the triplet−triplet annihilation rate is much larger than the spontaneous reverse intersystem crossing rate k'_{isc}, which explains the observation that the contrast is independent of excitation power. This regime was not achieved for MEH−PPV under the experimental conditions; higher excitation powers are required. The time-ensemble fluorescence intensity decays from an initial value to a steady-state value, reflecting a steady-state triplet exciton concentration that is due to rapid triplet−triplet annihilation.

The technique described in this paper basically provides data analogous to those from the autocorrelation experiments that have been described earlier. In fact, the quantitative information that has been obtained by both techniques is in very good

agreement. The advantage of the modulation technique is that the data are more straightforward to interpret and less prone to artifacts such as background luminescence and detector afterpulsing.

Acknowledgment. We greatly acknowledge support of this research by the National Science Foundation and the Robert A. Welch Foundation.

References and Notes

(1) Kohle, A.; Wilson, J. S.; Friend, R. H. *Adv. Mater.* **2002**, *14*, 701.
(2) Baldo, M. A.; O'Brien, D. F.; Thompson, M. E.; Forrest, S. R. *Phys. Rev. B* **1999**, *60*, 14422.
(3) Cao, Y.; Parker, I. D.; Yu, G.; Zhang, C.; Heeger, A. J. *Nature* **1999**, *397*, 414.
(4) Wilson, J. S.; Dhoot, A. S.; Seeley, A.; Khan, M. S.; Kohler, A.; Friend, R. H. *Nature* **2001**, *413*, 828.
(5) Wohlgenannt, M.; Jiang, X. M.; Vardeny, Z. V.; Janssen, R. A. J. *Phys. Rev. Lett.* **2002**, *88*, 197401.
(6) Shuai, Z.; Ye, A.; Beljonne, D.; Silbey, R. J.; Bredas, J. L. *Synth. Met.* **2001**, *121*, 1637.
(7) Ho, P. K. H.; Kim, J. S.; Burroughes, J. H.; Becker, H.; Li, S. F. Y.; Brown, T. M.; Cacialli, F.; Friend, R. H. *Nature* **2000**, *404*, 481.
(8) Beljonne, D.; Ye, A. J.; Shuai, Z.; Bredas, J. L. *Adv. Funct. Mater.* **2004**, *14*, 684.
(9) Barzda, V.; Vengris, M.; Valkunas, L.; Grondelle, R. v.; Amerongen, H. v. *Biochemistry* **2000**, *39*, 10468.
(10) Hofkens, J.; Schroeyers, W.; Loos, D.; Cotlet, M.; Kohn, F.; Vosch, T.; Maus, M.; Herrmann, A.; Mullen, K.; Gensch, T.; De Schryver, F. C. *Spectrochim. Acta, Part A* **2001**, *57*, 2093.
(11) Tinnefeld, P.; Buschmann, V.; Weston, K. D.; Sauer, M. *J. Phys. Chem. A* **2003**, *107*, 323.
(12) Hofkens, J.; Cotlet, M.; Vosch, T.; Tinnefeld, P.; Weston, K. D.; Ego, C.; Grimsdale, A.; Mullen, K.; Beljonne, D.; Bredas, J. L.; Jordens, S.; Schweitzer, G.; Sauer, M.; De Schryver, F. *Proc. Natl. Acad. Sci. U.S.A.* **2003**, *100*, 13146.
(13) Higgins, R. W. T.; Monkman, A. P.; Nothofer, H. G.; Scherf, U. *Appl. Phys. Lett.* **2001**, *79*, 857.
(14) Hale, G. D.; Oldenburg, S. J.; Halas, N. J. *Phys. Rev. B* **1997**, *55*, 16069.
(15) Hertel, D.; Bassler, H.; Guentner, R.; Scherf, U. *J. Chem. Phys.* **2001**, *115*, 10007.
(16) Rothe, C.; Monkman, A. P. *Phys. Rev. B* **2003**, *68*, 075208.
(17) Hino, Y.; Kajii, H.; Ohmori, Y. *Org. Electron.* **2004**, *5*, 265.
(18) Baldo, M. A.; Adachi, C.; Forrest, S. R. *Phys. Rev. B* **2000**, *62*, 10967.
(19) Adachi, C.; Baldo, M. A.; Forrest, S. R. *J. Appl. Phys.* **2000**, *87*, 8049.
(20) Baldo, M. A.; O'Brien, D. F.; You, Y.; Shoustikov, A.; Sibley, S.; Thompson, M. E.; Forrest, S. R. *Nature* **1998**, *395*, 151.
(21) Moerner, W. E.; Orrit, M. *Science* **1999**, *283*, 1670.
(22) Kulzer, F.; Orrit, M. *Annu. Rev. Phys. Chem.* **2004**, *55*, 585.
(23) Ambrose, W. P.; Goodwin, P. M.; Jett, J. H.; Van Orden, A.; Werner, J. H.; Keller, R. A. *Chem. Rev.* **1999**, *99*, 2929.
(24) Nie, S.; Zare, R. *Annu. Rev. Biophys. Biomol. Struct.* **1997**, *26*, 567.
(25) Xie, X. S.; Trautman, J. K. *Annu. Rev. Phys. Chem.* **1998**, *49*, 441.
(26) Summers, M. A.; Robinson, M. R.; Bazan, G. C.; Buratto, S. K. *Chem. Phys. Lett.* **2002**, *364*, 542.
(27) Kim, H. D.; Nienhaus, G. U.; Ha, T.; Orr, J. W.; Williamson, J. R.; Chu, S. *Proc. Natl. Acad. Sci. U.S.A.* **2002**, *99*, 4284.
(28) Mehta, A. D.; Rief, M.; Spudich, J. A.; Smith, D. A.; Simmons, R. M. *Science* **1999**, *283*, 1689.
(29) Talaga, D. S.; Lau, W. L.; Roder, H.; Tang, J.; Jia, Y.; DeGrado, W. F.; Hochstrasser, R. M. *Proc. Natl. Acad. Sci. U.S.A.* **2000**, *97*, 13021.
(30) Cotlet, M.; Masuo, S.; Luo, G. B.; Hofkens, J.; Van der Auweraer, M.; Verhoeven, J.; Mullen, K.; Xie, X. L. S.; De Schryver, F. *Proc. Natl. Acad. Sci. U.S.A.* **2004**, *101*, 14343.
(31) Lippitz, M.; Hubner, C. G.; Christ, T.; Eichner, H.; Bordat, P.; Herrmann, A.; Mullen, K.; Basche, T. *Phys. Rev. Lett.* **2004**, *92*, 103001.
(32) Vandenbout, D. A.; Yip, W. T.; Hu, D. H.; Fu, D. K.; Swager, T. M.; Barbara, P. F. *Science* **1997**, *277*, 1074.
(33) Yu, J.; Hu, D. H.; Barbara, P. F. *Science* **2000**, *289*, 1327.
(34) Hu, D.; Yu, J.; Barbara, P. *J. Am. Chem. Soc.* **1999**, *121*, 6936.
(35) Bartko, A. P.; Dickson, R. M. *J. Phys. Chem. B* **1999**, *103*, 3053.
(36) Huser, T.; Yan, M.; Rothberg, L. J. *Proc. Natl. Acad. Sci. U.S.A.* **2000**, *97*, 11187.
(37) Sartori, S. S.; De Feyter, S.; Hofkens, J.; Van der Auweraer, M.; De Schryver, F.; Brunner, K.; Hofstraat, J. W. *Macromolecules* **2003**, *36*, 500.
(38) Muller, J. G.; Lemmer, U.; Raschke, G.; Anni, M.; Scherf, U.; Lupton, J. M.; Feldmann, J. *Phys. Rev. Lett.* **2003**, *91*, 267403.
(39) Ronne, C.; Tragardh, J.; Hessman, D.; Sundstrom, V. *Chem. Phys. Lett.* **2004**, *388*, 40.
(40) Wang, C. F.; White, J. D.; Lim, T. L.; Hsu, J. H.; Yang, S. C.; Fann, W. S.; Peng, K. Y.; Chen, S. A. *Phys. Rev. B* **2003**, *67*, 035202.
(41) Yu, J.; Lammi, R. K.; Gesquiere, A. J.; Barbara, P. F. *J. Phys. Chem. B* **2005**, *109*, 10025.
(42) Yip, W.-T.; Hu, D.; Yu, J.; Vanden Bout, D. A.; Barbara, P. F. *J. Phys. Chem. A* **1998**, *102*, 7564.
(43) Hu, D. H.; Yu, J.; Wong, K.; Bagchi, B.; Rossky, P. J.; Barbara, P. F. *Nature* **2000**, *405*, 1030.